Radio Science, Volume 26, Number 5, Pages 1245–1249, September–October 1991

Wind and reflectivity fields around fronts observed with a VHF radar

Peter T. May,[1,2] *Mamoru Yamamoto,*[3] *Shoichiro Fukao,*[3] *Toru Sato,*[4] *Susumu Kato,*[3] *and Toshitaka Tsuda*[3]

(Received November 9, 1989; revised October 9, 1990; accepted October 17, 1990.)

The wind and VHF radar reflectivity fields around frontal zones are examined. While even weak upper level baroclinic zones can be seen in both the reflectivity and wind fields, the reflectivity signature of low level fronts may be obscured. Humidity terms dominate the refractive index gradient in the lower troposphere and can mask the enhancement of the gradient as a result of the stable frontal layers.

1. INTRODUCTION

Mesosphere-stratosphere-troposphere (MST) radars and wind profilers operating in the VHF band, at frequencies around 50 MHz, have observed enhanced signal levels in beams pointed to the zenith. The magnitude of the enhancements seems to be correlated with stability allowing the detection of the tropopause [e.g., *Rottger and Liu*, 1978; *Gage and Green*, 1979] and upper frontal boundaries [e.g., *Rottger*, 1979; *Rottger and Schmidt*, 1981; *Larsen and Rottger*, 1982, 1983, 1984]. *Tsuda et al.* [1988] have shown quantitatively that profiles of radar reflectivity follow profiles of the square of the generalized refractive index gradient M^2. However, below about 500 mbar, M^2 is dominated by humidity terms, and it is suggested here that the enhanced reflectivity associated with low level fronts may often be masked. However, even weak upper level baroclinic zones can be seen in the reflectivity. An example using the middle and upper (MU) atmosphere radar in Japan is used as an illustration.

2. EQUIPMENT

The MU radar, located in Shigaraki, Japan (35°N, 138°E), about 45 km southeast of Kyoto, represents the state of the art for the wind profiler technology and MST radars. Comprehensive descriptions of the radar are given by *Kato et al.* [1984] and *Fukao et al.* [1985*a*, *b*]. The routine operation of the radar allows observations to be performed with five (or more) beam directions, essentially simultaneously, in this case, one beam directed to the zenith and four beams directed 10° from the zenith, to the north, east, south, and west. A range resolution of 150 m was used, and the time resolution was of the order of 1 min. The minimum observable altitude was about 1 km, and winds up to the lower stratosphere (~19 km) were measured.

A least squares fitting method was used to estimate the spectral moments and a precision of about 0.2 ms^{-1} is obtained for the vertical wind component [*Yamamoto et al.*, 1988] and therefore about 1.5 ms^{-1} for the horizontal wind components using a 1-min sample. Small-scale wind fluctuations limit the accuracy of the wind measurements to about 1.5 ms^{-1} [*May et al.*, 1989], even for hourly averages [*Strauch et al.*, 1987]. The data here are averaged over 12 consecutive 1-min soundings using a consensus averaging technique [*Fischler and Bolles*, 1981]. Other effects such as thin scattering layers can introduce errors, but these errors are generally small below the jetstream [*May et al.*, 1988].

3. OBSERVATIONS

A shallow cold front associated with a midlatitude cyclone 600 km to the northeast passed over Shigaraki at around 1500 UTC (local midnight) on January 23, 1987. The cross section using observations from the standard observing network and surface chart (Figure 1) clearly show the presence of a relatively weak low level front associated with

[1] Cooperative Institute for Research in the Environmental Sciences (CIRES), University of Colorado, Boulder.
[2] Now at BMRC, Melbourne, Australia.
[3] Radio Atmospheric Science Center, Kyoto University, Uji, Kyoto, Japan.
[4] Department of Electrical Engineering, Kyoto University, Uji, Kyoto, Japan.

Paper number 91RS00964.
0048-6604/91/91RS-00964$08.00

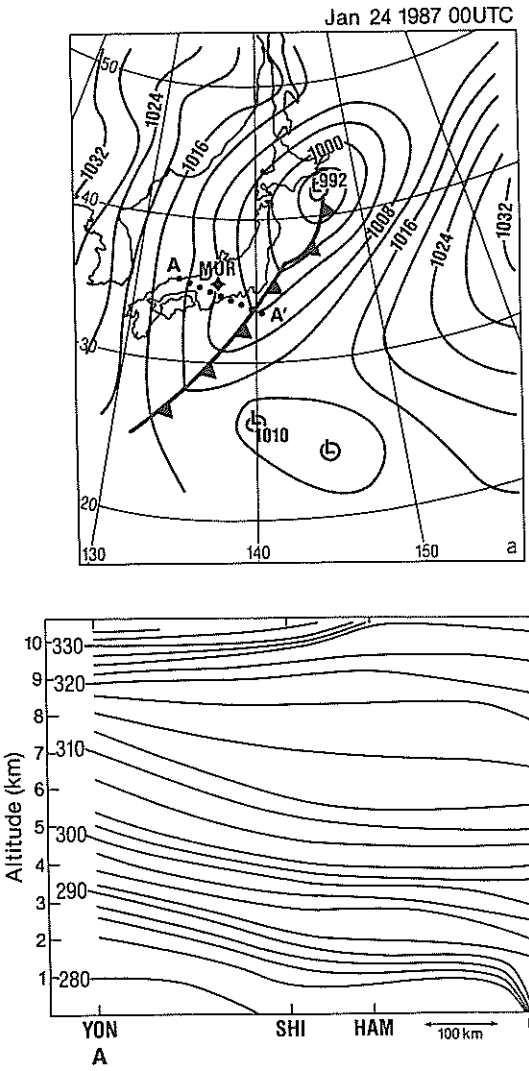

Fig. 1. (*a*) Surface chart showing the analyzed cold front associated with the low-pressure system over Hokaido. The line A-A′ shows the line used to objectively analyze (*b*) a cross section of the frontal system showing the potential temperature structure through the front. The stations used along A-A′ are Yonago (YON), Shionomisaki (SHI), Hamamatsu (HAM), and Hachijojima (HAC).

the low pressure cell to the northeast. The tropopause appears to slope downward to the west. There was a cold air outbreak behind the front, a common occurrence with cold fronts near Japan during the winter [*GARP*, 1981]. The cold air behind the front was about 3 km deep, and there was significant rainfall (~8 mm/hr) at the radar site for about 4 hours following the frontal passage.

The skew-T plot taken from a radiosonde

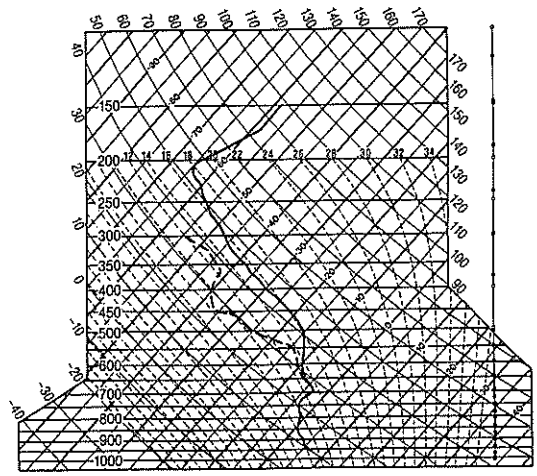

Fig. 2. Skew-T plot from a radiosonde launch from the radar site at 1900 UTC, about 4 hours after the frontal passage. Note the frontal inversion at 700 mbar (~3 km) and the tropopause at 210 mbar (~11 km).

launched from the radar site at 1900 UTC, some 4 hours after the frontal passage (Figure 2) clearly shows a well-defined frontal temperature inversion between 2.6 and 2.9 km, corresponding closely to the height of the enhanced low level vertical shear layer measured by the radar. The cold air below the inversion was saturated, but there was also significant moisture aloft. The profile is stable above the inversion up to at least 500 mbar, as was also seen in the cross-section, with a deep layer close to dry adiabatic above. The tropopause height was about 11 km.

Figure 3 shows the wind profiles and radar reflectivity field observed by the radar. The reflectivity is from the zenith pointing radar beam. Every other wind observation in time and height is plotted (i.e., 1/4 of the observations) so that the plot is not too cluttered. The passage of the low level front is clearly seen as the winds veered slightly with time and weakened about local midnight. Regions where the vertical gradient of the wind

$$\left[\left(\frac{du}{dz}\right)^2+\left(\frac{dv}{dz}\right)^2\right]^{1/2}$$

is greater than 10 ms^{-1} km^{-1} are shaded. The enhanced vertical wind shear highlights the frontal passage. A possible upper level baroclinic zone can be seen descending from about 11.5 km down to 7 km between 1800 and 2000 UTC highlighted by

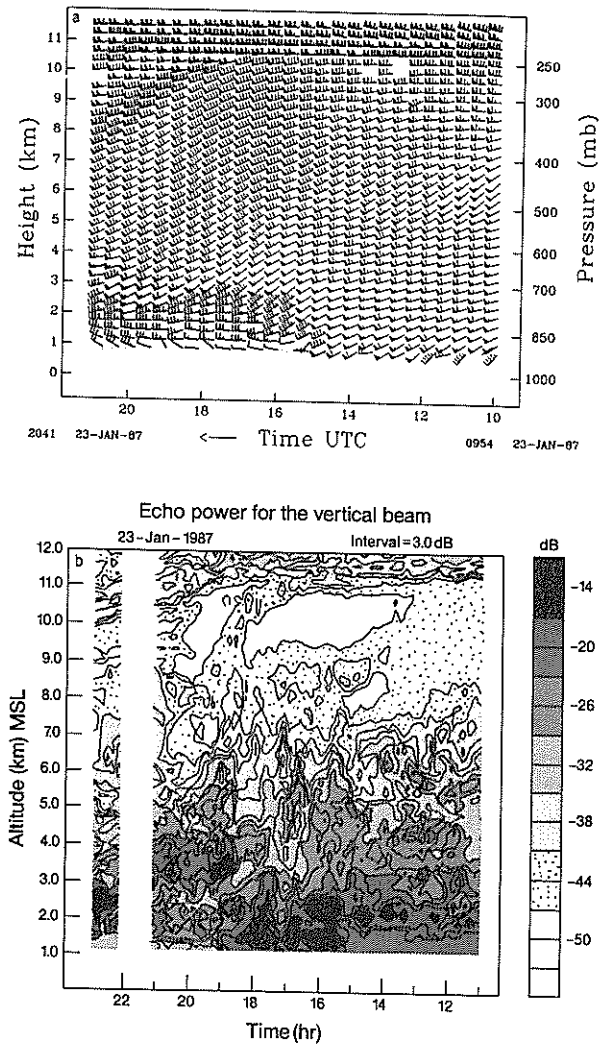

Fig. 3. (*a*) Wind profiles measured around the passage of the surface front. Areas where the vertical wind shear exceeded 10 ms^{-1} km^{-1} are shaded. A flag represents 25 ms^{-1}, barb 5 ms^{-1}, and a half barb 2.5 ms^{-1}. (*b*) Contours of radar reflectivity measured by a zenith pointing beam about the frontal passage. Note the confused field around the front and the thin layer of enhanced reflectivity extending down from the tropopause at 1900.

enhanced wind shear. The reflectivity field shows a layer with about a 3-dB enhancement in signal strength coincident with the upper shear layer. However, the reflectivity field below 4 km is very convoluted and no clear signal associated with the surface front can be distinguished. The tropopause can be clearly seen at about 11 km in the reflectivity.

4. DISCUSSION

The wind field clearly shows the lower tropospheric frontal zone. Locating frontal surfaces and shear zones are capabilities which make wind profilers such useful tools for meteorology [*Shapiro et al.*, 1984]. The vertical shear associated with the lower tropospheric front was well organized and strong (up to 20 ms^{-1} km^{-1}) below about 3.5 km. The upper level vertical shear zone associated with a possible upper level baroclinic zone is nearly masked in the flag and barbs plot but is clearly delineated by the wind gradient field. Backing of the wind with height in the lower frontal zone indicates cold advection below 3 km (assuming approximate geostrophic balance) within the cold air mass behind the front; consistent with the cold air outbreak. A significant question is whether the reflectivity observed by a VHF zenith pointing radar beam can be used to locate and track frontal surfaces.

Various studies have shown that the backscattered power from a vertically pointed beam is related to M^2 [e.g., *Gage and Green*, 1978; *Green and Gage*, 1980]. In particular, *Tsuda et al.* [1988] showed quantitatively a 1-1 correlation between the echo power and M^2. M may be written as

$$M = -79\times10^{-6}\frac{P}{T}\frac{\partial \ln \theta}{\partial z} \cdot \left\{1+\frac{15500q}{T}\left\{1-0.5\left(\frac{\partial \ln q}{\partial z}\right)\Big/\left(\frac{\partial \ln \theta}{\partial z}\right)\right\}\right\}$$

where P is the pressure, T is the temperature in Kelvin, θ is the potential temperature, q is the specific humidity, and z is the altitude. Note that M^2 can be represented by three terms: a stability term, a humidity gradient term, and a crossed term. If we can neglect the terms involving the humidity, then M^2, and hence backscattered power, is proportional to the square of the gradient of the potential temperature. This is the physical principle which allows tropopause detection and suggests the possibility of sensing the static stability associated with frontal interfaces. Figure 4 shows the profile of M^2 with the humidity contribution included and the profile of M^2 ignoring humidity calculated from the radiosonde launched after the frontal passage where the profiles were smoothed over 50 m. There are several significant features. First, the humidity term is some 10 dB greater than the dry term below about

6 km. Although the dry term has a substantial peak at the frontal inversion, the overall M^2 profile actually has a minimum there. The structure of humidity fields are more complex than temperature fields, and sharp gradients are not necessarily confined to frontal regions although they may be large there. This explains why some low level fronts may not be detected in the radar reflectivity (for example, cold fronts observed by the Adelaide VHF radar during the Australian Cold Fronts Program showed no reflectivity signature). Several profiles of echo power are shown in Figure 5 along with the height of the surface front estimated from the wind shear. Note that there is little correlation between the frontal height and echo power, i.e., the height of the front is distributed between minima and maxima in the power profile. Above about 7 km, M^2 is dominated by its dry term, although M^2 is small several kilometers below the tropopause because the air is only slightly statically stable. The gross features of the M^2 profile agree with a 12-min average power profile obtained by the radar, although there are differences in detail due to the spatial separation of the observations and averaging, both in height and time of the radar reflectivity. For example, the tropopause stands out clearly, as it does in the radar reflectivity data. A small enhancement associated with the upper level layer is visible, but it is its time-height continuity in the radar reflectivity as seen in the reflectivity contour

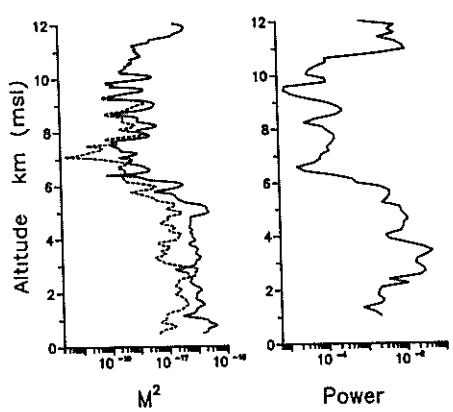

Fig. 4. (*a*) Profile of M^2 calculated from the radiosonde ascent. The temperature and humidity profiles were smoothed over 50 m for the calculations. The dashed curve is the M^2 that would be obtained with zero humidity, and the solid curve is calculated using the full expression for M^2. (*b*) Profile of the backscattered power detected by the radar averaged from 1900–1912 UTC.

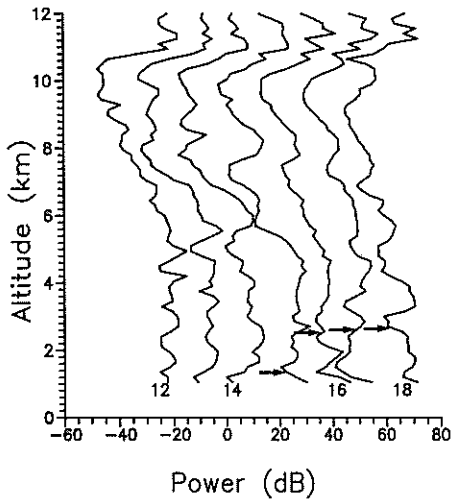

Fig. 5. Seven profiles of echo power averaged over 15 min. Samples from the beginning of each hour from 1200 UTC up to 1800 UTC are shown. Successive profiles are offset by 15 dB. The height of the frontal surface is marked by the arrows.

plot which makes it obvious. Thus the layers' enhanced reflectivity indicates a statically stable layer, and the coincident wind shear indicates a horizontal temperature gradient, so that the layer may be identified as a weak upper level baroclinic zone. Note that this feature cannot be identified in the cross section, possibly because of the poor spatial resolution of the network.

Some theoretical studies [*Gage et al.*, 1985] have suggested that the enhanced backscatter from the zenith should be proportional to $M^2E(2k)$, where $E(2k)$ is the intensity of fluctuations with a scale of half the radar wavelength. This makes the observed proportionality to M^2 somewhat puzzling since, at heights where humidity contributions are unimportant, M is related to the static stability, so that regions of large M^2 may be altitudes where $E(2k)$ is suppressed. One possible solution [*Tsuda et al.*, 1988] is that the variations with height of the M^2 profile are so large (factors of 10–100 about layers) that they dominate the fluctuations of $E(2k)$. Large wind shears around fronts can also result in turbulent regions despite high static stability [*Shapiro*, 1978].

5. CONCLUSIONS

Wind profilers operating in the VHF band are clearly useful tools for observing the wind field

around frontal regions [e.g., *Shapiro et al.*, 1984], but it is shown here that the radar reflectivity may be insensitive for locating low level fronts because of the dominance of the humidity terms in M^2. Fronts may be associated with large humidity contrasts, but the humidity microstructure is often more complex and the humidity terms in M^2 may even have the opposite signs to the enhancements as a result of stable temperature gradients causing some cancellation. On the other hand, even weak upper level features, mostly missed by conventional techniques have been observed in the radar reflectivity. Thus a combination of shear detection and reflectivity are an excellent tool for detecting upper level baroclinic zones. These weak upper front associated structures are a topic for future work, since they appear to be common (for example, see another example by *Tsuda et al.* [1988]) and therefore may be important for many problems such as troposphere/stratosphere exchange [e.g., *Shapiro*, 1974].

Acknowledgments. Part of this work was performed while one of us (P.T.M.) was visiting the Radio Atmospheric Science Centre of Kyoto University. He was supported by the Japan Society for the Promotion of Science and the Australian Academy of Science. The MU Radar belongs to and is operated by the Radio Atmospheric Science Center of Kyoto University.

REFERENCES

Fischler, M. A., and R. C. Bolles, Random sample consensus: A paradigm for model fitting with applications to image analysis and automated cartography, *Commun. ACM*, *24*, 381–395, 1981.

Fukao, S., T. Sato, T. Tsuda, S. Kato, K. Wakasugi, and T. Makihara, The MU Radar with an active phased array system, 1, Antenna and power amplifiers, *Radio Sci.*, *20*, 1155–1168, 1985*a*.

Fukao, S., T. Tsuda, T. Sato, S. Kato, K. Wakasugi, and T. Makihara, The MU Radar with an active phased array system 2, In-house equipment, *Radio Sci.*, *20*, 1169–1176, 1985*b*.

Gage, K. S., and J. L. Green, Evidence for specular reflection from monostatic VHF radar observations of the stratosphere, *Radio Sci.*, *13*, 991–1001, 1978.

Gage, K. S., and J. L. Green, Tropopause detection by partial specular reflection using VHF radar, *Science*, *203*, 1238–1240, 1979.

Gage, K. S., W. L. Ecklund, and B. B. Balsey, A modified Fresnel scattering model for the parameterization of Fresnel returns, *Radio Sci.*, *20*, 1493–1502, 1985.

GARP, Scientific results of the air mass transformation experiment (AMTEX), *GARP Publ. Ser.*, *24*, 237 pp., 1981.

Green, J. L., and K. S. Gage, Observations of stable layers in the troposphere and stratosphere using VHF radar, *Radio Sci.*, *15*, 395–405, 1980.

Kato, S., T. Ogawa, T. Tsuda, I. Kimura, and S. Fukao, The middle and upper atmosphere radar: First results using a partial system, *Radio Sci.*, *19*, 1475–1484, 1984.

Larsen, M. F., and J. Rottger, VHF and UHF Doppler radars as tools of synoptic research, *Bull. Am. Meteorol. Soc.*, *63*, 996–1008, 1982.

Larsen, M. F., and J. Rottger, Comparison of tropopause height and frontal boundary locations based on radar and radiosonde data, *Geophys. Res. Lett.*, *10*, 325–328, 1983.

Larsen, M. F., and J. Rottger, Observations of frontal zone structures with a VHF Doppler radar and radiosondes, in *MAP Handbook*, vol. 14, edited by S. A. Bowhill and B. Edwards, pp. 7–13, SCOSTEP Secretariat, University of Illinois, Urbana, 1984.

May, P. T., S. Fukao, T. Tsuda, T. Sato, and S. Kato, The effect of thin scattering layers on the determination of wind by Doppler radars, *Radio Sci.*, *23*, 83–95, 1988.

May, P. T., T. Sato, M. Yamamoto, S. Kato, S. Fukao, and T. Tsuda, Errors in the determination of winds by Doppler radars, *J. Atmos. Oceanic Technol.*, *6*, 235–242, 1989.

Rottger, J., VHF radar observations of a frontal passage, *J. Appl. Meteorol.*, *18*, 85–91, 1979.

Rottger, J., and C. H. Liu, Partial reflection and scattering of VHF radar signals from the clear atmosphere, *Geophys. Res. Lett.*, *5*, 357–360, 1978.

Rottger, J., and G. Schmidt, Characteristics of frontal zones determined from SA VHF radar measurements, paper presented at 20th Conference on Radar Meteorology, Am. Meteorol. Soc., Boston, Mass.

Shapiro, M. A., A multiple structured frontal zone–jet stream system as revealed by a meteorologically instrumented aircraft, *Mon. Weather Rev.*, *102*, 244–253, 1974.

Shapiro, M. A., Further evidence of the messoscale and turbulent structure of upper level jet stream–frontal systems, *Mon. Weather Rev.*, *106*, 1100–1111, 1978.

Shapiro, M. A., T. Hample, and D. W. Van de Kamp, Radar wind profiler observations of fronts and jet streams, *Mon. Weather Rev.*, *112*, 1263–1266, 1984.

Strauch, R. G., B. L. Weber, A. S. Frisch, C. G. Little, D. A. Merritt, K. P. Moran, and D. C. Welsh, The precision and relative accuracy of wind profiler measurements, *J. Atmos. Oceanic Technol.*, *4*, 563–571, 1987.

Tsuda, T., P. T. May, T. Sato, S. Kato, and S. Fukao, Simultaneous observations of reflection echoes and refractive index gradient in the troposphere and lower stratosphere, *Radio Sci.*, *23*, 655–665, 1988.

Yamamoto, M., T. Sato, P. T. May, T. Tsuda, S. Fukao, and S. Kato, Estimation error of spectral parameters of mesosphere-stratosphere-troposphere radars obtained by least squares fitting method and its lower bound, *Radio Sci.*, *23*, 1013–1022, 1988.

S. Fukao, S. Kato, T. Tsuda, and M. Yamamoto, Radio Atmospheric Science Center, Kyoto University, Uji, Kyoto, Japan.

P. T. May, BMRC, GPO Box 1289K, Melbourne, Victoria 3001, Australia.

T. Sato, Department of Electrical Engineering, Kyoto University, Uji, Kyoto, Japan.